

ICOS-Fc as innovative immunomodulatory approach to counteract inflammation and organ injury in sepsis

1 Gustavo Ferreira Alves¹, Ian Stoppa², Eleonora Aimaretti³, Chiara Monge⁴, Raffaella
2 Mastrocola³, Elisa Porchietto⁵, Giacomo Einaudi⁵, Debora Collotta¹, Ilaria Bertocchi¹, Elena
3 Boggio², Casimiro Luca Gigliotti², Nausicaa Clemente², Manuela Aragno³, Daniel Fernandes⁶,
4 Carlo Cifani⁵, Christoph Thiemermann⁷, Chiara Dianzani⁴, Umberto Dianzani^{2†}, Massimo
5 Collino^{1*†}

6 ¹Department of Neurosciences (Rita Levi Montalcini), University of Turin, Turin, Italy

7 ²Department of Health Sciences, Università del Piemonte Orientale, Novara Italy

8 ³Department of Clinical and Biological Sciences, University of Turin, Turin, Italy

9 ⁴Department of Drug Science and Technology, University of Turin, Turin, Italy

10 ⁵Pharmacology Unit, School of Pharmacy, University of Camerino, Camerino, Italy

11 ⁶Department of Pharmacology, Federal University of Santa Catarina, Florianópolis, Brazil

12 ⁷William Harvey Research Institute, Bart's and The London School of Medicine and Dentistry,
13 Queen Mary University of London, London, United Kingdom

14

15 † Both authors contributed equally.

16 * Correspondence:

17 Massimo Collino,

18 Department of Neurosciences (Rita Levi Montalcini)

19 Corso Raffaello 30, 10125 Torino, Italy

20 E-mail address: massimo.collino@unito.it

21

22 **Keywords:** sepsis, inflammation, ICOS (inducible co-stimulatory molecule), cecal ligation and
23 puncture, osteopontin (OPN)

24 ABSTRACT

25 Inducible T cell co-stimulator (ICOS), an immune checkpoint protein expressed on activated T cells
26 and its unique ligand, ICOSL, which is expressed on antigen-presenting cells and non-hematopoietic
27 cells, have been extensively investigated in the immune response. Recent findings showed that a
28 soluble recombinant form of ICOS (ICOS-Fc) can act as an innovative immunomodulatory drug as
29 both antagonist of ICOS and agonist of ICOSL, modulating cytokine release and cell migration to
30 inflamed tissues. Although the ICOS-ICOSL pathway has been poorly investigated in the septic
31 context, a few studies have reported that septic patients have reduced ICOS expression in whole
32 blood and increased serum levels of osteopontin (OPN), that is another ligand of ICOSL. Thus, we
33 investigated the pathological role of the ICOS-ICOSL axis in the context of sepsis and the potential
34 protective effects of its immunomodulation by administering ICOS-Fc in a murine model of sepsis.

35 Polymicrobial sepsis was induced by cecal ligation and puncture (CLP) in five-month-old male wild-
36 type (WT) C57BL/6, ICOS^{-/-}, ICOSL^{-/-} and OPN^{-/-} mice. One hour after the surgical procedure, either
37 CLP or Sham (control) mice were randomly assigned to receive once ICOS-Fc, ^{F119S}ICOS-Fc, a
38 mutated form incapable to bind ICOSL, or vehicle intravenously. Organs and plasma were collected
39 24 h after surgery for analyses. When compared to Sham mice, WT mice that underwent CLP
40 developed within 24 h a higher clinical severity score, a reduced body temperature, an increase in
41 plasma cytokines (TNF- α , IL-1 β , IL-6, IFN- γ and IL-10), liver injury (AST and ALT) and kidney
42 (creatinine and urea) dysfunction. Administration of ICOS-Fc to WT CLP mice reduced all of these
43 abnormalities caused by sepsis. Similar beneficial effects were not seen in CLP-mice treated with
44 ^{F119S}ICOS-Fc. Treatment of CLP-mice with ICOS-Fc also attenuated the sepsis-induced local
45 activation of FAK, P38 MAPK and NLRP3 inflammasome. ICOS-Fc seemed to act at both sides of
46 the ICOS-ICOSL interaction, as the protective effect was lost in septic knockout mice for the ICOS
47 or ICOSL genes, whereas it was maintained in OPN knockout mice. Collectively, our data show the
48 beneficial effects of pharmacological modulation of the ICOS-ICOSL pathway in counteracting the
49 sepsis-induced inflammation and organ dysfunction.

50

51 INTRODUCTION

52 Sepsis is a life-threatening medical emergency characterized by a complex interplay of pro- and anti-
53 inflammatory host responses, resulting in multiple organ dysfunction that can ultimately lead to death
54 [1]. Currently, deaths from sepsis correspond to nearly 20% of all deaths worldwide, and there is still
55 no specific treatment available [2]. The inducible T cell co-stimulator (ICOS, also known as CD278)
56 belongs to the CD28 family of co-stimulatory immunoreceptors. It is a type I transmembrane
57 glycoprotein whose expression is rapidly upregulated upon T cells activation [3]. ICOS binds to its
58 unique ligand (ICOSL, also known as CD275 or B7h), a member of the B7 family highly expressed
59 on antigen-presenting cells (APCs) and non-hematopoietic cells under inflammatory stimuli [4][5].
60 Thus far, the role of ICOS-ICOSL interaction has been poorly investigated in sepsis, although recent
61 findings report that ICOS expression is reduced in whole blood of septic patients [6], and that
62 reduced ICOS levels are strongly associated with organ dysfunction [7]. To date, it is very well
63 documented that the ICOS-ICOSL axis may display bidirectional effects. On the one hand, ICOS
64 triggering modulates cytokine production in activated T cells and contributes to T regulatory (Treg)
65 cells differentiation and survival [8][9]. Given the fact that both animals and septic patients have an
66 increased percentage of circulating Treg cells [10][11][12], it is suggestive that ICOS triggering may
67 play a role in the septic immunosuppressive status. On the other hand, ICOSL triggering by ICOS
68 may exert anti-inflammatory effects via responses, such as modulating the maturation and migration
69 of macrophage and dendritic cells and the endothelial cell adhesiveness [13].

70 Recently, another ligand for ICOSL has been identified, osteopontin (OPN), an inflammatory
71 mediator that binds to ICOSL in an alternative binding domain to that used by ICOS. Intriguingly,
72 ICOS and OPN exert different and often opposite effects upon ICOSL triggering since OPN
73 stimulates, whereas ICOS inhibits, migration of several cell types and tumor angiogenesis
74 [14][15][16]. Conventionally, a soluble recombinant form of ICOS (ICOS-Fc) has been designed by
75 fusing a cloned extracellular portion of human or mouse ICOS with an Fc IgG1 portion and this
76 molecule has been shown to trigger ICOSL thus promoting down-stream responses [17].

77 *In vitro*, ICOS-Fc inhibits adhesiveness of endothelial cells toward polymorphonuclear cells and
78 tumor cells and migration of endothelial cells and tumor cells [15]. These ICOS-Fc effects can also

79 be recorded in dendritic cells (DC), along with modulated cytokine release and antigen cross-
80 presentation in class I major histocompatibility complex molecules [13], while in osteoclasts, ICOS-
81 Fc inhibits differentiation and function [18]. *In vivo*, ICOS-Fc inhibits tumor growth and metastasis,
82 development of osteoporosis, liver damage induced by acute inflammation following treatment with
83 CCl₄, and it favors skin wound healing [19][18][20][21]. Nevertheless, little is known about the
84 molecular mechanism(s) involved in ICOSL-mediated inflammatory response. The p38 MAPK, a
85 well-known mediator that drives inflammation through upregulation of several pro-inflammatory
86 cytokines such as TNF- α and IL-6 [22], and the NOD-like receptor protein 3 (NLRP3)
87 inflammasome, able to induce the release of IL-1 β and IL-18 and promote cell death by pyroptosis
88 [23], are two of the most well characterized signaling pathways involved in the activation of the
89 cytokine storm that contributes to organ dysfunction during sepsis. Furthermore, their
90 pharmacological or genetic inhibition has been shown to reduce sepsis-related mortality [22][24].
91 Finally, a non-receptor protein kinase namely Focal adhesion kinase (FAK) has been recently
92 reported to signal inflammation downstream of the Toll-like receptor 4 upon lipopolysaccharide
93 (LPS) challenge in macrophages and lung tissues [25]. Therefore, here we investigated, for the first
94 time, the pathological role of ICOS-ICOSL axis in the context of sepsis, its impact on selective
95 inflammatory pathways and the potential protective effects of its immunomodulation by
96 administering ICOS-Fc in an experimental model of sepsis.

97

98 **MATERIAL AND METHODS**

99 **Animals and Ethical statement**

100 Inbred wild-type (WT, C57BL/6) mice, ICOSL knockout mice (ICOSL^{-/-}, B6.129P2-*Icosl*^{tm1Mak/J}),
101 ICOS knockout mice (ICOS^{-/-}, B6.129P2-*Icos*^{tm1Mak/J}) and OPN knockout mice (OPN^{-/-},
102 B6.129S6(Cg)-*Spp1*^{tm1Blh/J}) were purchased from Envigo laboratories, (IT) and The Jackson
103 Laboratory (Bar Harbor, ME, USA). Mice were housed under standard laboratory conditions, such as
104 room temperature (25 \pm 2 °C) and light-controlled with free access to water and rodent chow for four
105 weeks prior starting the experimental procedures. All animal protocols reported in this study
106 followed the ARRIVE guidelines [26] and the recommendations for preclinical studies of sepsis
107 provided by the MQTiPSS [27] The procedures were approved by the University's Institutional
108 Ethics Committee as well as the National Authorities (Protocol number: 855/2021).

109 **Cecal Ligation and Puncture (CLP)-induced sepsis model**

110 Polymicrobial sepsis was carried out by CLP surgery in male, five-month-old mice. Mice were
111 initially placed in an anaesthesia chamber (3% isoflurane -IsoFlo, Abbott Laboratories – delivered in
112 oxygen 0.4 L/min), then kept under anaesthesia throughout surgery with 2% isoflurane delivered in
113 oxygen 0.4 L/min via a nosecone. The body temperature was maintained at 37 °C through a
114 homoeothermic blanket and constantly monitored by a rectal thermometer. Briefly, a mid-line
115 laparotomy (~1.0 cm) was performed in the abdomen, exposing the cecum. The cecum was then
116 totally ligated just below the ileocecal valve and a G-21 needle was used to puncture the ligated
117 cecum in a single through-and-through manner. A small amount (droplet, ~3mm) of fecal content
118 was released from the cecum which was carefully relocated into the peritoneum. Sham mice
119 underwent the same surgical procedure, but without CLP. All animals received Carprofen (5 mg/kg,
120 s.c.) as an analgesic agent and resuscitation fluid (0.9% NaCl, 50 mL/kg, s.c.) at 37 °C. Mice were
121 constantly monitored post-surgical and then placed back into fresh clean cages.

122 At 24 h, body temperature and a clinical score to assess symptoms consistent with murine sepsis
123 were recorded blindly. The following 6 criteria were used for the clinical score: lethargy,
124 piloerection, tremors, periorbital exudates, respiratory distress and diarrhea. An observed clinical
125 score >3 was considered as severe sepsis, while a score between 3 and 1 was considered as moderate
126 sepsis [28].

127 **Study design**

128 Seventy-two mice were randomized into eight groups (9 mice per group): Sham + Vehicle, CLP +
129 Vehicle, CLP + ICOS-Fc, CLP + ^{F119S}ICOS-Fc, CLP ICOSL^{-/-} + Vehicle, CLP ICOS^{-/-} + Vehicle,
130 CLP ICOS^{-/-} + ICOS-Fc and OPN^{-/-} + Vehicle. Treatment was given once one hour after surgery,
131 where mice received either ICOS-Fc (100 µg each), ^{F119S}ICOS-Fc (100 µg each) or Vehicle (PBS, pH
132 7.4, 100 µl each) by intravenous injection (Figure 1).

133 **Blood collection and organ harvesting**

134 Twenty-four h after surgery all mice were anesthetized with isoflurane (3%) delivered in oxygen (0.4
135 L/min) and euthanized by cardiac exsanguination. Whole blood was withdrawn from each mouse in
136 vials (EDTA 17.1 µM/mL) and plasma content was obtained after centrifugation (13,000 g, 10 min at
137 R.T.). Organ samples (liver and kidney) were harvested and placed in cryotubes which were snap
138 frozen in liquid nitrogen for storage at freezer -80 °C. The samples were then analyzed in a blinded
139 fashion (Figure 1).

140 **Biomarkers of organ injury and systemic inflammation**

141 Plasma samples were used to measure systemic levels of aspartate aminotransferase (AST) (#7036)
142 and alanine aminotransferase (ALT) (#7018) (as markers of hepatocellular injury), creatinine (#7075)
143 and urea (#7144) (as markers of renal dysfunction) using colorimetric clinical assay kits (FAR
144 Diagnostics, Verona, Italy) according to the manufacturer's instructions. Systemic cytokine levels
145 were determined in plasma using the Luminex suspension bead-based multiplexed Bio-Plex Pro™
146 Mouse Cytokine Th17 Panel A 6-Plex (#M6000007NY) assay (Bio-Rad, Kabsketal, Germany).
147 The cytokines (IL-1β, IL-6, TNF-α, IFN-γ, IL-17 and IL-10) were measured following the
148 manufacturer's instructions.

149 **Myeloperoxidase (MPO) activity analysis**

150 MPO activity analysis was carried out in liver and kidney samples as previously described[29].
151 Tissue samples (~100 mg) were homogenized (1:5 w-v) in 20 mM PBS (pH 7.4) and then
152 centrifuged at 4 °C (13,000 g, 10 min). Pellets were resuspended in 500 µL of
153 hexadecyltrimethylammonium bromide buffer (0.5% HTAB in 50 mM PBS, pH 6.0). A second
154 centrifugation at 4 °C (13,000 g, 10 min) was performed and the supernatants (30 µL) were assessed
155 for MPO activity by measuring spectrophotometrically (650 nm) the H₂O₂-dependent oxidation of
156 3,3',5,5'-tetramethylbenzidine (TMB). Bicinchoninic acid (BCA) protein assay (Pierce
157 Biotechnology Inc., Rockford, IL, USA) was used to quantify the protein content in the final
158 supernatant. MPO activity was expressed as optical density (O.D.) at 650 nm per mg of protein.

159 **Western blot analysis**

160 Semi-quantitative immunoblot technique was carried out in hepatic and renal tissue samples as
161 previously described [30]. Total proteins were extracted from 50 mg of each tissue and the total

162 content was quantified using BCA protein method following the manufacturer's instructions. Briefly,
163 total proteins (50 µg/well) were separated by 8 and 10% sodium dodecyl sulphate-polyacrylamide gel
164 electrophoresis (SDS-PAGE) and transferred to a polyvinylidene difluoride (PVDF) membrane,
165 which was then blocked with 5% non-fat dry mil prepared in TBS-T buffer for 1 h at RT, followed
166 by incubation with primary antibodies at the dilution 1:1000., rabbit anti-Thr¹⁸⁰/anti-Tyr¹⁸² p38 (Cell
167 Signaling #9211); rabbit anti-total p38 (Cell Signaling #9212); mouse anti-NRLP3 (Adipogen- AG-
168 20B-0014-C100); rabbit anti-Caspase-1 (Cell Signaling #24232); rabbit anti-Tyr³⁹⁷ FAK (Cell
169 Signaling #3283); rabbit anti-total FAK (Cell Signaling #3285). The membranes were then incubated
170 with a secondary antibody conjugated with horseradish peroxidase (HRP) at the dilution 1:10000 for
171 1 h at RT (anti-mouse or anti-rabbit, Cell Signaling #7076 and #7074, respectively). Afterwards, the
172 membranes were stripped and incubated with rabbit anti-β-actin (Cell Signaling #4970). Immune
173 complexes were visualized by chemiluminescence and the densitometric analysis was performed
174 using Bio-Rad Image Lab Software 6.0.1. Results were normalized to sham bands.

175 **Statistical Analysis data presentation**

176 Sample size was determined on the basis of prior power calculations using G-Power 3.1™ software
177 [31]. Data are expressed as dot plots (for each mouse) and as mean ± S.E.M of 9 mice per group.
178 Shapiro-Wilk and Bartlett tests were used to verify data distribution and the homogeneity of
179 variances, respectively. The statistical analysis was performed by one-way ANOVA, followed by
180 Bonferroni's post-hoc test. Data not normally distributed, a non-parametric statistical analysis was
181 applied through Kruskal-Wallis followed by Dunn's post hoc-test as indicated in the figure legends.
182 Statistical significance was set at P < 0.05. Statistical analysis was performed using GraphPad
183 Prism® software version 7.05 (San Diego, California, USA).

184

185 **Materials**

186 Unless otherwise stated, all reagents were purchased from the Sigma-Aldrich Company Ltd. (St.
187 Louis, Missouri, USA).

188

189 **RESULTS**

190 **ICOS-Fc-mediated immunomodulation attenuates clinical status and organ injury/dysfunction** 191 **triggered by sepsis**

192 Sepsis was induced by CLP in WT mice treated with vehicle, ICOS-Fc or ^{F119S}ICOS-Fc (unable to
193 bind ICOSL) and clinical scores and body temperature were recorded after 24 h. Moreover, sepsis
194 was induced in mice deficient for ICOS, ICOSL, or OPN to assess the role the endogenous molecules
195 of the ICOS/ICOSL/OPN system. Finally, a group of ICOS-deficient mice received ICOS-Fc
196 treatment to evaluate the effect of the drug in the absence of the endogenous ICOS.

197 Results showed that, as expected, CLP-induced sepsis in WT mice led to a higher clinical severity
198 score (Figure 2a) when compared to Sham WT mice, which was also associated with lower body
199 temperature (Figure 2b). Intriguingly, treatment with ICOS-Fc improved both clinical score and
200 hypothermia in WT septic mice, whereas treatment with ^{F119S}ICOS-Fc had no effect (Figures 2a, b).
201 Analysis of CLP knockout mice showed that ICOS^{-/-} and ICOSL^{-/-} mice showed similar clinical

202 scores and decreased body temperatures as WT mice, whereas OPN^{-/-} mice developed milder sepsis,
203 with lower clinical scores and higher body temperature than WT mice. In ICOS^{-/-} mice, treatment
204 with ICOS-Fc induced similar positive effects as in WT mice (Figures 2a, b).

205 To investigate organ injury or dysfunction, plasma levels of ALT, AST, creatinine and urea were
206 evaluated in these mice. Figure 3 shows that results mirrored those shown in Fig.2: CLP-induced
207 sepsis caused striking increase of ALT, AST, creatinine and urea levels in WT type mice, and these
208 levels were decreased by treatment with ICOS-Fc, but not F^{119S}ICOS-Fc. Levels of these markers
209 were increased also in CLP ICOS^{-/-} and ICOSL^{-/-} mice and urea levels were even higher in ICOS^{-/-}
210 than in WT mice. In CLP ICOS^{-/-} mice, treatment with ICOS-Fc significantly decreased all these
211 markers. In CLP OPN^{-/-} mice, levels of these markers were significantly lower than in CLP WT mice.

212

213 **ICOS-Fc administration modulates experimental sepsis-induced cytokine storm**

214 The 6 cytokines were measured systemically in plasma samples by using a multiplex array. Figure 4
215 shows that, in WT mice, CLP-induced sepsis led to a cytokine storm with significant increase of
216 levels of IL-1 β , IL-6, IL-10, TNF- α , IFN- γ and a slight not significant increase of IL-17 compared to
217 Sham mice. Administration of ICOS-Fc to WT CLP mice induced a significant decrease of IL-1 β and
218 TNF- α , whereas F^{119S}ICOS-Fc had no effect. Levels of IL-1 β , IL-6, IL-10, TNF- α , and IFN- γ were
219 also increased in CLP ICOS^{-/-} and ICOSL^{-/-} mice at levels similar to those observed in CLP WT mice.
220 Moreover, CLP ICOSL^{-/-} mice showed higher levels of IL-17 than Sham mice, and CLP ICOS^{-/-} mice
221 displayed higher levels of TNF- α and, especially, IL-10 than CLP WT mice. The CLP ICOS^{-/-} mice
222 treated with ICOS-Fc significantly decreased levels of IL-1 β , IL-6 and IL-10 compared to the
223 untreated counterparts. In CLP OPN^{-/-} mice, the increase of these cytokines was in general moderate,
224 with levels of IL-6, IL-10, TNF- α and IFN- γ higher than in Sham mice, and levels of IL-1 β and IL-6
225 lower than in CLP WT mice.

226

227 **ICOS-Fc treatment reduces sepsis-induced increase in MPO activity in the kidney**

228 MPO activity was assessed in the liver and kidney, as an indirect biomarker of leukocyte tissue
229 infiltration (Figure 5). When compared to Sham mice, CLP WT mice had increased MPO activity in
230 both liver and kidney samples, and MPO activity was significantly decreased by ICOS-Fc (but not
231 F^{119S}ICOS-Fc treatment) in the kidney, but not in the liver. In the liver, MPO activity was similarly
232 increased also in CLP ICOS^{-/-}, ICOSL^{-/-}, and OPN^{-/-} mice, and it was not modified by ICOS-Fc
233 treatment in CLP ICOS^{-/-} mice. In the kidney, MPO activity was increased in CLP ICOS^{-/-} and
234 ICOSL^{-/-} mice, and treatment with ICOS-Fc decreased MPO activity in CLP ICOS^{-/-} mice. By
235 contrast, CLP OPN^{-/-} mice showed lower MPO levels in the kidney than CLP WT mice.

236

237 **ICOS-Fc treatment reduces local FAK/p38 signalling and NLRP3 inflammasome** 238 **activation in septic mice**

239

240 In order to better elucidate the molecular mechanism underlying the beneficial effects evoked by
241 ICOS-Fc administration, we focused on WT mice investigating the changes in some signaling

242 cascades, previously documented to be affected by the ICOS-ICOSL axis and, at the same time,
243 known to exert key role in sepsis pathogenesis. Western blot analysis showed that CLP mice showed
244 significant increase of the phosphorylation of FAK at Tyr³⁹⁷ and p38 MAPK at Thr¹⁸⁰/Tyr¹⁸² in both
245 hepatic (Figures 6a, c) and renal (Figures 6b, d) tissues, when compared to Sham mice. Interestingly,
246 mice treatment with ICOS-Fc significantly attenuated the degree of phosphorylation of FAK/p38 axis
247 in both tissues, thus suggesting reduced activation of these signaling pathways (Figures 6a-d).

248 We then assessed the activation of the inflammasome, by evaluating the expression of NLRP3 and
249 cleaved caspase-1 in both liver and kidney samples (Figures 6e-h). Results showed that, in both
250 tissues, CLP-induced sepsis significantly increased both molecules, and the increase was inhibited by
251 mice treatment with ICOS-Fc (Figures 6e-h).

252

253 **DISCUSSION**

254 Currently, most research on sepsis is focused on blocking the initial hyperinflammation, which in
255 turn has resulted in promising outcomes. However, recent reports showed and that both pro- and anti-
256 inflammatory responses occur immediately and simultaneously after the onset of sepsis and most
257 patients who survive this initial hyperinflammatory phase develop an immunosuppressive phase that
258 can progress to late deaths [1][32][33]. Among the main causes of death in this immunosuppressive
259 phase, the failure to control a primary infection and/or secondary hospital-acquired infections stands
260 out [34]. In the present study we report for the first time that ICOS-ICOSL axis may play a role in
261 regulation of uncontrolled inflammation and organ injury induced by sepsis and that treatment of
262 septic mice with ICOS-Fc may represent a novel immunomodulatory pharmacological approach that
263 can simultaneously counteract both sepsis-induced hyperinflammation and immunosuppression.

264 These findings were obtained by evoking polymicrobial sepsis in either WT mice and knockout mice
265 for ICOS, ICOSL and OPN genes. As expected, severe sepsis (score ≥ 3) was observed in vehicle-
266 treated septic mice, suggesting potential late deaths, since the clinical scoring system is used as a
267 surrogate marker of mortality. This detrimental effect was also associated with low body temperature
268 (~ 27 °C), as similarly, hypothermia is another surrogate marker of mortality, as a 5 °C decrease over
269 time or < 30 °C has also been shown to predict death in CLP-induced septic mice. [35]. Moreover,
270 septic mice showed liver and kidney damage, displayed by increase of plasma AST/ALT and
271 creatinine/urea levels, respectively, which is in line with the notion that sepsis can cause multiple
272 organ failure including hepatocellular injury and renal dysfunction.

273 Intriguingly, treatment with ICOS-Fc substantially ameliorated the clinical picture by significantly
274 decreasing all these parameters of sepsis. The effect was specific since no protection was detected
275 following administration of ^{F119S}ICOS-Fc (a mutated form of ICOS-Fc carrying a phenylalanine-to-
276 serine substitution at position 119).

277 Theoretically, the protective activity of ICOS-Fc might be ascribed to a twofold mechanism, i.e. on
278 the one hand to the inhibition of the endogenous ICOS activity and, on the other hand, to triggering
279 of the endogenous ICOSL. However, the effectiveness of ICOS-Fc not only in WT mice but also in
280 ICOS^{-/-} mice, lacking the endogenous ICOS, strongly suggest that the main protective effect on sepsis
281 is due to triggering of ICOSL, which is in line with previous works showing that ICOSL triggering
282 by ICOS-Fc elicits several anti-inflammatory activities both *in vitro* and *in vivo* [13][15][16][19].

283 These results are in keeping also with recent findings showing that ICOS-Fc protects against liver
284 damage through a shift of pro-inflammatory monocyte-derived macrophages to an anti-inflammatory
285 phenotype [20]. In parallel, the direct renoprotective effect triggered by ICOS-Fc treatment is
286 supported by a recent study showing a key role of ICOSL in preventing early kidney disease,
287 possibly through a selective binding to podocyte $\alpha\text{v}\beta\text{3}$ integrin, in which ICOSL serves as an $\alpha\text{v}\beta\text{3}$ -
288 selective antagonist that maintains adequate glomerular filtration [36].

289 The use of knockout mice highlighted that, in sepsis, a key role may be played by OPN as all the
290 above septic parameters were significantly decreased in $\text{OPN}^{-/-}$ mice, so that OPN deficiency
291 mirrored the effect of ICOS-Fc in WT mice. This finding is in line with data showing that, in
292 humans, OPN levels are increased in sepsis [37] and OPN might be involved in the sepsis
293 pathogenesis, possibly by supporting IL-6 secretion [38]. Moreover, several reports showed that
294 ICOS-Fc inhibits several proinflammatory activities of OPN *in vitro* and *in vivo* [16][37][39][40].
295 Our findings are in keeping also with recent data showing that macrophage-derived OPN promotes
296 glomerular injury in an experimental model of inflammatory and progressive kidney disease [41].
297 OPN is an heavily phosphorylated extracellular protein, expressed and secreted by several cell types,
298 including macrophages, endothelial cells, dendritic cells and T-cells.. It can act as a cytokine
299 mediating several biological functions, including cell migration, adhesion, activation of inflammatory
300 cells, and modulation of T cell activation supporting differentiation of proinflammatory type 1 (Th1)
301 and type 17 (Th17) Th cells [42].

302 Analysis of plasmatic cytokines showed that, in all mouse strains, sepsis was accompanied by
303 increase of IL-1 β , IL-6, IL-10, TNF- α and IFN- γ . Moreover, increase of TNF- α and, especially, IL-
304 10 was particularly striking in $\text{ICOS}^{-/-}$ mice, which may point out that ICOS deficiency causes a
305 dysregulation of activation of M1 and M2 macrophages. However, treatment with ICOS-Fc
306 significantly decreased IL-1 β and TNF- α in WT mice and IL-1 β , IL-6 and IL-10 in $\text{ICOS}^{-/-}$ mice
307 indicating that ICOS-Fc substantially downmodulates the cytokine storm in sepsis. In $\text{OPN}^{-/-}$ mice,
308 increase of these cytokines was in general moderate, with a significant decrease of IL-1 β and IL-6, in
309 line with the mild sepsis developed by these mice.

310 Among the main inflammatory pathways activated during sepsis, we report a local (liver and kidney)
311 overactivation of the FAK and p38 MAPK pathways in CLP mice. Previously, we have shown that
312 the FAK pathway mediates inflammation through p38 MAPK and that this inflammatory axis plays a
313 role in exacerbating inflammation [28]. Activation of this axis promotes increased
314 expression/secretion of pro-inflammatory cytokines such as TNF- α , IL-6, IL-1 β and IL-17, which in
315 turn contribute to the cytokine storm and multiple organ failure (MOF) associated with sepsis [43].
316 Intriguingly, treatment of septic mice with ICOS-Fc significantly attenuated FAK and p38 MAPK
317 phosphorylation, thus reducing their activation during septic insult, with a following impact on the
318 development of the above-mentioned cytokine storm. These findings are in accordance with previous
319 studies focused on tumor cell migration, whose treatment with ICOS-Fc reduces FAK and p38
320 MAPK activation both *in vitro* and *in vivo* [15][19]. As we and other have recently shown, FAK
321 activation may also affect the overexpression and activation of another peculiar inflammatory
322 pathway, NLRP3 inflammasome complex [28][44]. Thus, we wondered here whether ICOS-Fc could
323 also infer with this cross-talk mechanism linking FAK to NLRP3 activation within the septic context.
324 We report here that experimental sepsis led to an overactivation of the NLRP3 complex and
325 consequent activation of its downstream mediator caspase-1, which were significantly reduced by
326 treatment with ICOS-Fc, thus leading to reduced systemic release of IL-1 β . In addition to the impact
327 on the aforementioned inflammatory pathways, ICOS-Fc administration seems to directly affect
328 leukocyte migration in CLP mice, as documented by the changes in MPO activity, a well-known

329 biomarker of neutrophil infiltration, in both liver and kidney homogenates [45]. Specifically, we
330 documented that the sepsis-induced increase in MPO activity in renal tissues, was significantly
331 counteracted by ICOS-Fc treatment. This effect, on the other hand, was absent when CLP mice were
332 treated with ^{F119S}ICOS-Fc. Intriguingly, increased MPO activity was recorded in liver homogenates
333 from septic mice, regardless of drug treatment or genetic intervention, when compared to Sham mice.
334 Despite ICOS-Fc has been shown to reduce the migration of polymorphonuclear cells into inflamed
335 tissues [15], these discrepant events observed in liver and kidney tissue may be the result of different
336 levels of ICOSL expression. This finding corroborates a previous study reporting that hepatocytes did
337 not express ICOSL, when compare to other organs, such as the kidney [46]. Thus, suggesting that the
338 hepatic protection induced by ICOS-Fc in septic mice is mainly due to a local and systemic
339 resolution of inflammation rather than a reduction in leukocyte infiltration. A schematic
340 representation summarizing the role of ICOS-ICOSL axis in the pathogenesis of sepsis and the
341 protective effects of ICOS-Fc following sepsis-induced multiple organ failure is shown in Figure 7.

342 Despite the originality of our findings, we are aware of several limitations of our study, including the
343 lack of extension of these findings to other important functional organs related to MOF during sepsis,
344 such as the lungs and the cardiac tissue, along with the lack of analysis suggestive of the direct effect
345 of ICOS-Fc treatment in preventing immunosuppression. Albeit the *in vivo* protocol described here is
346 in accordance with the main recommendations provided by MQTiPSS consensus guidelines [27], we
347 are not authorized to perform a survival study to assess the long-term effect of ICOS-Fc due to
348 ethical reasons. Thus, further studies are needed to extend the clinical relevance of our findings as
349 well as to gain a better insight into the safety profile of the proposed drug treatment.

350

351 **CONCLUSIONS**

352 In conclusion, we demonstrate here, for the first time, that the ICOS-ICOSL axis plays a crucial role
353 in the development of systemic inflammation and organ damage induced by a clinically relevant
354 sepsis model. These findings were confirmed by an exacerbation of septic injury in mice knockout
355 for the ICOS and ICOSL genes. Interestingly, we also documented its druggability by showing
356 protection when ICOS-Fc, a recombinant protein which act as an antagonist of ICOS and an agonist
357 of ICOSL, was administered during sepsis. The beneficial effects of this innovative pharmacological
358 approach are likely due to a potential cross-talk mechanisms involving the FAK-p38-NLRP3
359 inflammasome axis. A greater understanding of the molecular basis of ICOS-Fc-mediated effects is
360 needed to harness its actions as a potentially powerful immunomodulatory tool for counteracting
361 inflammation and organ injury in sepsis.

362

363 **CONFLICT OF INTEREST**

364 The authors declare that the research was conducted in the absence of any commercial or financial
365 relationships that could be construed as a potential conflict of interest.

366

367 **AUTHOR CONTRIBUTIONS**

368 G.F.A., C.D., U.D. and M.C. conceived and designed the experiments. G.F.A., I.S., E.A., C.M.,
369 R.M., E.P., G.E., D.C., N.C. performed the experiments. G.F.A., E.A., C.M., R.M., I.B., E.B.,
370 C.L.G., N.C., M.A., D.F., C.T., C.C., C.D., U.D. and M.C. analyzed the data. G.F.A., C.D., U.D.,
371 C.T. and M.C writing - review and editing. All authors have read and agreed to the published version
372 of the manuscript.

373

374 **FUNDING**

375 The Università degli Studi di Torino has supported and funded this work (Ricerca Locale 2020 and
376 2021) and by the Associazione Italiana Ricerca sul Cancro (IG20714), Milan Italy.

377

378 **DATA AVAILABILITY STATEMENT**

379 The dataset supporting this study are available on request to the corresponding author, without undue
380 reservation. **ACKNOWLEDGMENT**

381 Parts of the figure 7 were drawn by using pictures from Servier Medical Art. Servier Medical Art by
382 Servier is licensed under a Creative Commons Attribution 3.0 Unported License
383 (<https://creativecommons.org/licenses/by/3.0/>).

384

385 **REFERENCES**

- 386 [1] R. S. Hotchkiss, G. Monneret, and D. Payen, “Sepsis-induced immunosuppression: From
387 cellular dysfunctions to immunotherapy,” *Nat. Rev. Immunol.*, vol. 13, no. 12, pp. 862–874,
388 Dec. 2013, doi: 10.1038/nri3552.
- 389 [2] K. E. Rudd *et al.*, “Global , regional , and national sepsis incidence and mortality , 1990 –
390 2017 : analysis for the Global Burden of Disease Study,” *Lancet*, vol. 395, no. 10219, pp. 200–
391 211, 2020, doi: 10.1016/S0140-6736(19)32989-7.
- 392 [3] A. Hutloff *et al.*, “ICOS is an inducible T-cell co-stimulator structurally and functionally
393 related to CD28,” *Nature*, vol. 100, no. 1981, pp. 263–266, 1999, doi: 10.1038/16717.
- 394 [4] S. K. Yoshinaga *et al.*, “T-cell co-stimulation through B7RP-1 and ICOS,” *Nature*, vol. 1, pp.
395 827–832, 1999, doi: 10.1038/45582.
- 396 [5] M. M. Swallow, J. J. Wallin, and W. C. Sha, “B7h , a Novel Costimulatory Homolog of B7.1
397 and B7.2 , Is Induced by TNFa,” *Immunity*, vol. 11, pp. 423–432, 1999, doi: 10.1016/s1074-
398 7613(00)80117-x.
- 399 [6] P. Möhnle *et al.*, “MicroRNAs 143 and 150 in whole blood enable detection of T-cell
400 immunoparalysis in sepsis,” *Mol. Med.*, vol. 24, no. 1, pp. 1–14, 2018, doi: 10.1186/s10020-
401 018-0056-z.
- 402 [7] R. Menéndez *et al.*, “Simultaneous depression of immunological synapse and endothelial

- 403 injury is associated with organ dysfunction in community-acquired pneumonia,” *J. Clin. Med.*,
404 vol. 8, no. 9, pp. 1–10, 2019, doi: 10.3390/jcm8091404.
- 405 [8] Y. Burmeister *et al.*, “ICOS Controls the Pool Size of Effector-Memory and Regulatory T
406 Cells,” *J. Immunol.*, vol. 180, pp. 774–782, 2008, doi: 10.4049/jimmunol.180.2.774.
- 407 [9] Q. Chen *et al.*, “ICOS signal facilitates Foxp3 transcription to favor suppressive function of
408 regulatory T cells,” *Int. J. Med. Sci.*, vol. 15, no. 7, pp. 666–673, 2018, doi:
409 10.7150/ijms.23940.
- 410 [10] Y. Luan, C. Yin, Q. Qin, N. Dong, X. Zhu, and Z. Sheng, “Effect of Regulatory T Cells on
411 Promoting Apoptosis of T Lymphocyte and Its Regulatory Mechanism in Sepsis,” *J. Interf.*
412 *CYTOKINE Res.*, vol. 35, no. 12, pp. 969–980, 2015, doi: 10.1089/jir.2014.0235.
- 413 [11] K. SAITO *et al.*, “Sepsis is Characterized by the Increases in Percentages of Circulating CD4
414 + CD25 + Regulatory T Cells and Plasma Levels of Soluble CD25,” *J. Exp. Med.*, vol. 216,
415 pp. 61–68, 2008, doi: 10.1620/tjem.216.61.
- 416 [12] F. Leng, J. Liu, Z. Liu, J. Yin, and H.-P. Qu, “Increased proportion of CD4 D CD25 D Foxp3
417 D regulatory T cells during early-stage sepsis in ICU patients,” *J. Microbiol. Immunol. Infect.*,
418 vol. 46, no. 5, pp. 338–344, 2013, doi: 10.1016/j.jmii.2012.06.012.
- 419 [13] S. Occhipinti *et al.*, “Triggering of B7h by the ICOS Modulates Maturation and Migration of
420 Monocyte-Derived Dendritic Cells,” *J. Immunol.*, vol. 190, no. 3, pp. 1125–1134, 2013, doi:
421 10.4049/jimmunol.1201816.
- 422 [14] S. A. Lund and C. M. Giachelli, “The role of osteopontin in inflammatory processes,” *J. Cell*
423 *Commun. Signal.*, vol. 3, pp. 311–322, 2009, doi: 10.1007/s12079-009-0068-0.
- 424 [15] C. Dianzani *et al.*, “B7h Triggering Inhibits Umbilical Vascular Endothelial Cell Adhesiveness
425 to Tumor Cell Lines and Polymorphonuclear Cells,” *J. Immunol.*, vol. 185, pp. 3970–3979,
426 2010, doi: 10.4049/jimmunol.0903269.
- 427 [16] D. Raineri *et al.*, “Osteopontin binds ICOSL promoting tumor metastasis,” *Commun. Biol.*,
428 vol. 3, no. 615, pp. 1–15, 2020, doi: 10.1038/s42003-020-01333-1.
- 429 [17] R. Di Niro *et al.*, “Construction of miniantibodies for the in vivo study of human autoimmune
430 diseases in animal models,” *BMC Biotechnol.*, vol. 7, pp. 1–10, 2007, doi: 10.1186/1472-
431 6750-7-46.
- 432 [18] C. L. Gigliotti *et al.*, “ICOS-Ligand Triggering Impairs Osteoclast Differentiation and
433 Function In Vitro and In Vivo,” *J. Immunol.*, vol. 197, no. 10, pp. 3905–3916, 2016, doi:
434 10.4049/jimmunol.1600424.
- 435 [19] C. Dianzani *et al.*, “B7h Triggering Inhibits the Migration of Tumor Cell Lines,” *J. Immunol.*,
436 vol. 192, no. 10, pp. 4921–4931, 2014, doi: 10.4049/jimmunol.1300587.
- 437 [20] N. N. Ramavath *et al.*, “Inducible T-Cell Costimulator Mediates Lymphocyte/Macrophage
438 Interactions During Liver Repair,” *Front. Immunol.*, vol. 12, pp. 1–14, 2021, doi:
439 10.3389/fimmu.2021.786680.

- 440 [21] I. Stoppa *et al.*, “ICOSL Stimulation by ICOS-Fc Accelerates Cutaneous Wound Healing In
441 Vivo,” *Int. J. Mol. Sci.*, vol. 23, pp. 1–12, 2022.
- 442 [22] A. W. O’Sullivan, J. H. Wang, and H. P. Redmond, “NF- κ B and P38 MAPK Inhibition
443 Improve Survival in Endotoxin Shock and in a Cecal Ligation and Puncture Model of Sepsis
444 in Combination With Antibiotic Therapy,” *J. Surg. Res.*, vol. 152, no. 1, pp. 46–53, 2009, doi:
445 10.1016/j.jss.2008.04.030.
- 446 [23] D. C. Cornelius *et al.*, “NLRP3 inflammasome inhibition attenuates sepsis-induced platelet
447 activation and prevents multi-organ injury in cecal-ligation puncture,” *PLoS One*, vol. 15, no.
448 6 June, pp. 1–15, 2020, doi: 10.1371/journal.pone.0234039.
- 449 [24] S. Lee *et al.*, “NLRP3 inflammasome deficiency protects against microbial sepsis via
450 increased lipoxin B4 synthesis,” *Am. J. Respir. Crit. Care Med.*, vol. 196, no. 6, pp. 713–726,
451 2017, doi: 10.1164/rccm.201604-0892OC.
- 452 [25] X. Chen *et al.*, “FAK mediates LPS-induced inflammatory lung injury through interacting
453 TAK1 and activating TAK1-NF κ B pathway,” *Cell Death Differ.*, vol. 13, no. 589, pp. 1–12,
454 2022, doi: 10.1038/s41419-022-05046-7.
- 455 [26] N. P. du Sert *et al.*, “The arrive guidelines 2.0: Updated guidelines for reporting animal
456 research,” *PLoS Biol.*, vol. 18, no. 7, pp. 1–12, 2020, doi: 10.1371/journal.pbio.3000410.
- 457 [27] M. F. Osuchowski *et al.*, “Minimum quality threshold in pre-clinical sepsis studies (mqtips):
458 An international expert consensus initiative for improvement of animal modeling in sepsis,”
459 *Shock*, vol. 50, no. 4, pp. 377–380, 2018, doi: 10.1097/SHK.0000000000001212.
- 460 [28] G. F. Alves *et al.*, “Pharmacological Inhibition of FAK-Pyk2 Pathway Protects Against Organ
461 Damage and Prolongs the Survival of Septic Mice,” *Front. Immunol.*, vol. 13, pp. 1–14, 2022,
462 doi: 10.3389/fimmu.2022.837180.
- 463 [29] V. Kovalski *et al.*, “Protective role of cGMP in early sepsis,” *Eur. J. Pharmacol.*, vol. 807, no.
464 May, pp. 174–181, 2017, doi: 10.1016/j.ejphar.2017.05.012.
- 465 [30] K. K. Nandra, M. Collino, M. Rogazzo, R. Fantozzi, N. S. A. Patel, and C. Thiemermann,
466 “Pharmacological preconditioning with erythropoietin attenuates the organ injury and
467 dysfunction induced in a rat model of hemorrhagic shock,” *DMM Dis. Model. Mech.*, vol. 6,
468 no. 3, pp. 701–709, 2013, doi: 10.1242/dmm.011353.
- 469 [31] F. Faul, E. Erdfelder, A.-G. Lang, and A. Buchner, “G*Power 3: A flexible statistical power
470 analysis program for the social, behavioral, and biomedical sciences,” *Behav. Res. Methods*,
471 vol. 39, no. 2, pp. 175–191, 2007, doi: 10.3758/bf03193146.
- 472 [32] P. Tsirigotis, S. Chondropoulos, K. Gkirkas, J. Meletiadis, and I. Dimopoulou, “Balanced
473 control of both hyper and hypo-inflammatory phases as a new treatment paradigm in sepsis,”
474 *J. Thorac. Dis.*, vol. 8, no. 5, pp. E312–E316, 2016, doi: 10.21037/jtd.2016.03.47.
- 475 [33] J. S. Boomer *et al.*, “Immunosuppression in patients who die of sepsis and multiple organ
476 failure,” *JAMA - J. Am. Med. Assoc.*, vol. 306, no. 23, pp. 2594–2605, 2011, doi:
477 10.1001/jama.2011.1829.

- 478 [34] G. P. Otto *et al.*, “The late phase of sepsis is characterized by an increased microbiological
479 burden and death rate,” *Crit. Care*, vol. 15, no. 4, pp. 1–8, 2011, doi: 10.1186/cc10332.
- 480 [35] S. H. C. Mai *et al.*, “Body temperature and mouse scoring systems as surrogate markers of
481 death in cecal ligation and puncture sepsis,” *Intensive Care Med. Exp.*, vol. 6, no. 1, pp. 1–14,
482 2018, doi: 10.1186/s40635-018-0184-3.
- 483 [36] K. H. Koh *et al.*, “Nonimmune cell–derived ICOS ligand functions as a renoprotective $\alpha\beta 3$
484 integrin–selective antagonist,” *J. Clin. Invest.*, vol. 129, no. 4, pp. 1713–1726, 2019, doi:
485 10.1172/JCI123386.
- 486 [37] L. M. Castello *et al.*, “The role of osteopontin as a diagnostic and prognostic biomarker in
487 sepsis and septic shock,” *Cells*, vol. 8, no. 2, pp. 1–12, 2019, doi: 10.3390/cells8020174.
- 488 [38] T. Uchibori, K. Matsuda, T. Shimodaira, M. Sugano, T. Uehara, and T. Honda, “IL-6 trans-
489 signaling is another pathway to upregulate Osteopontin,” *Cytokine*, vol. 90, pp. 88–95, 2017,
490 doi: 10.1016/j.cyto.2016.11.006.
- 491 [39] Y. Hirano *et al.*, “Neutralization of osteopontin attenuates neutrophil migration in sepsis-
492 induced acute lung injury,” *Crit. Care*, vol. 19, no. 1, pp. 1–15, 2015, doi: 10.1186/s13054-
493 015-0782-3.
- 494 [40] S. Fortis, R. G. Khadaroo, J. J. Haitzma, and H. Zhang, “Osteopontin is associated with
495 inflammation and mortality in a mouse model of polymicrobial sepsis,” *Acta Anaesthesiol.*
496 *Scand.*, vol. 59, no. 2, pp. 170–175, 2015, doi: 10.1111/aas.12422.
- 497 [41] J. Trostel *et al.*, “Disease different effects of global osteopontin and macrophage osteopontin
498 in glomerular injury,” *Am. J. Physiol. - Ren. Physiol.*, vol. 315, no. 4, pp. F759–F768, 2018,
499 doi: 10.1152/ajprenal.00458.2017.
- 500 [42] E. Boggio *et al.*, “Thrombin Cleavage of Osteopontin Modulates Its Activities in Human Cells
501 In Vitro and Mouse Experimental Autoimmune Encephalomyelitis In Vivo,” *J. Immunol. Res.*,
502 vol. 2016, pp. 1–13, 2016, doi: 10.1155/2016/9345495.
- 503 [43] H. Chaudhry *et al.*, “Role of cytokines as a double-edged sword in sepsis,” *In Vivo*
504 (*Brooklyn*), vol. 27, no. 6, pp. 669–684, 2013.
- 505 [44] I. C. Chung *et al.*, “Pyk2 activates the NLRP3 inflammasome by directly phosphorylating
506 ASC and contributes to inflammasome-dependent peritonitis,” *Sci. Rep.*, vol. 6, no. June, pp.
507 1–13, 2016, doi: 10.1038/srep36214.
- 508 [45] H. Yu *et al.*, “Myeloperoxidase instigates proinflammatory responses in a cecal ligation and
509 puncture rat model of sepsis,” *Am. J. Physiol. - Hear. Circ. Physiol.*, vol. 319, no. 3, pp.
510 H705–H721, 2020, doi: 10.1152/ajpheart.00440.2020.
- 511 [46] C. Wahl, P. Bochtler, L. Chen, R. Schirmbeck, and J. Reimann, “B7-H1 on Hepatocytes
512 Facilitates Priming of Specific CD8 T Cells But Limits the Specific Recall of Primed
513 Responses,” *Gastroenterology*, vol. 135, no. 3, pp. 980–988, 2008, doi:
514 10.1053/j.gastro.2008.05.076.

515

516 **FIGURE LEGENDS**

517 **Figure 1. Timeline of the experimental design to investigate the role of ICOS-Fc in sepsis.** Wild-
518 type mice and/or ICOSL, ICOS and OPN knockout mice were randomly selected to undergo either
519 Sham or CLP surgery. One hour later, mice received once either Vehicle (PBS, 100 μ L), ICOS-Fc
520 (100 μ g) or ^{F119S}ICOS-Fc (100 μ g) intravenously. At 24 h all parameters were analyzed.

521 **Figure 2. Role of the ICOS-ICOSL axis in the clinical status of experimental sepsis.** Wild-type
522 mice and/or ICOSL, ICOS and OPN knockout mice were randomly selected to undergo either Sham
523 or CLP surgery. One hour later, mice received once either Vehicle (PBS, 100 μ L), ICOS-Fc (100 μ g)
524 or ^{F119S}ICOS-Fc (100 μ g) intravenously. At 24 h, severity score [a] and body temperature [b] were
525 recorded. Data are expressed as dot plots (for each animal) and as mean \pm S.E.M of 9 mice per group.
526 Severity score was analyzed by a non-parametric test (Kruskal-Wallis) followed by Dunn's post hoc-
527 test, whereas a parametric test (one-way ANOVA) followed by Bonferroni's post hoc-test was used
528 for body temperature. *p<0.05 vs Sham + Vehicle; #p<0.05 vs CLP + Vehicle; &p<0.05 vs ICOS^{-/-} +
529 Vehicle.

530 **Figure 3. Effect of ICOS-ICOSL axis immunomodulation on sepsis-induced organ damage**
531 **biomarkers.** Wild-type mice and/or ICOSL, ICOS and OPN knockout mice were randomly selected
532 to undergo either Sham or CLP surgery. One hour later, mice received once either Vehicle (PBS, 100
533 μ L), ICOS-Fc (100 μ g) or ^{F119S}ICOS-Fc (100 μ g) intravenously. At 24 h, blood samples were
534 withdrawn from each mouse and plasma levels of alanine transaminase (ALT) [a], aspartate
535 transaminase (AST) [b], creatinine [c] and urea [d] were determined. Data are expressed as dot plots
536 (for each animal) and as mean \pm S.E.M of 9 mice per group. Statistical analysis was performed by
537 one-way ANOVA followed by Bonferroni's post hoc test. *p<0.05 vs Sham + Vehicle; #p<0.05 vs
538 CLP + Vehicle; &p<0.05 vs ICOS^{-/-} + Vehicle.

539 **Figure 4. Effect of ICOS-ICOSL axis immunomodulation on systemic cytokines during**
540 **experimental sepsis.** Wild-type mice and/or ICOSL, ICOS and OPN knockout mice were randomly
541 selected to undergo either Sham or CLP surgery. One hour later, mice received once either Vehicle
542 (PBS, 100 μ L), ICOS-Fc (100 μ g) or ^{F119S}ICOS-Fc (100 μ g) intravenously. At 24 h, blood samples
543 were withdrawn from each mouse and plasma levels of IL-1 β [a], IL-6 [b], TNF- α [c], IFN- γ [d], IL-
544 17 [e] and IL-10 [f] were determined. Data are expressed as dot plots (for each animal) and as mean
545 \pm S.E.M of 9 mice per group. Statistical analysis was performed by one-way ANOVA followed by
546 Bonferroni's post hoc test. *p<0.05 vs Sham + Vehicle; #p<0.05 vs CLP + Vehicle; &p<0.05 vs ICOS^{-/-}
547 + Vehicle.

548 **Figure 5. Effect of ICOS-ICOSL axis immunomodulation on sepsis-induced neutrophil (MPO**
549 **activity) infiltration.** Wild-type mice and/or ICOSL, ICOS and OPN knockout mice were randomly
550 selected to undergo either Sham or CLP surgery. One hour later, mice received once either Vehicle
551 (PBS, 100 μ L), ICOS-Fc (100 μ g) or ^{F119S}ICOS-Fc (100 μ g) intravenously. At 24 h, liver and kidney
552 samples were harvested. Through an *in vitro* assay, myeloperoxidase (MPO) activity was measured
553 in liver [a] and kidney [b]. Data are expressed as dot plots (for each animal) and as mean \pm S.E.M
554 of 6 mice per group. Statistical analysis was performed by one-way ANOVA followed by
555 Bonferroni's post hoc test. *p<0.05 vs Sham + Vehicle; #p<0.05 vs CLP + Vehicle; &p<0.05 vs ICOS^{-/-}
556 + Vehicle.

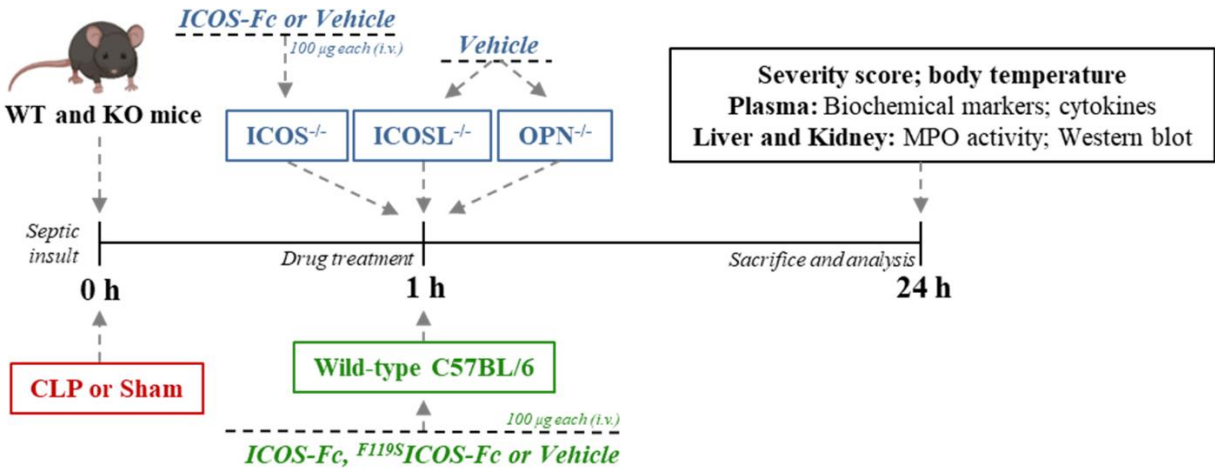
557

558 **Figure 6. Effect of ICOS-ICOSL axis immunomodulation on tissue inflammatory pathways**
559 **during experimental sepsis.** Wild-type mice and/or ICOSL, ICOS and OPN knockout mice were
560 randomly selected to undergo either Sham or CLP surgery. One hour later, mice received once either
561 Vehicle (PBS, 100 μ L), ICOS-Fc (100 μ g) or ^{F119S}ICOS-Fc (100 μ g) intravenously. At 24 h, liver
562 and kidney samples were harvested, and total proteins were extracted from them. Western blotting
563 analysis for phosphorylation of Tyr³⁹⁷ on FAK in the liver [a] and kidney [b] were normalized to
564 total FAK; Phosphorylation of Thr¹⁸⁰/Tyr¹⁸² on p38 in the liver [c] and kidney [d] were normalized to
565 total p38; NLRP3 expression in the liver [e] and kidney [f] were corrected against β -actin and
566 normalized using the Sham related bands; Cleaved caspase-1 expression in the liver [g] and kidney
567 [h] were corrected against β -actin and normalized using the Sham related bands. Densitometric
568 analysis of the bands are expressed as relative optical density (O.D.). Data are expressed as dot plots
569 (for each animal) and as mean \pm S.E.M of 4-5 mice per group. Statistical analysis was performed by
570 one-way ANOVA followed by Bonferroni's post hoc test. * $p < 0.05$ vs Sham + Vehicle; # $p < 0.05$ vs
571 CLP + Vehicle.

572 **Figure 7: Schematic representation on the role of ICOS-ICOSL axis in the pathogenesis of**
573 **sepsis.** Septic insult results in an imbalance in the ICOS-ICOSL axis, leading to bidirectional harmful
574 effects, where, on the one hand, the triggering of ICOS can induce immunosuppression, while, on the
575 other hand, the signaling pathway downstream of the ICOSL protein leads to overactivation of FAK-
576 p38-NLRP3 axis, promoting the transcription of pro-inflammatory genes, as well as the cleavage of
577 pro IL-1 β into IL-1 β and subsequent production of pro-inflammatory cytokines. Leukocyte
578 recruitment is also stimulated by the release of cytokines. Systemic hyperinflammation (cytokine
579 storm), along with polymorphonuclear cell recruitment, contributes to the onset of multiple organ
580 failure. Treatment with ICOS-Fc can attenuate sepsis-induced hyperinflammation and therefore MOF
581 to improve clinical outcomes.

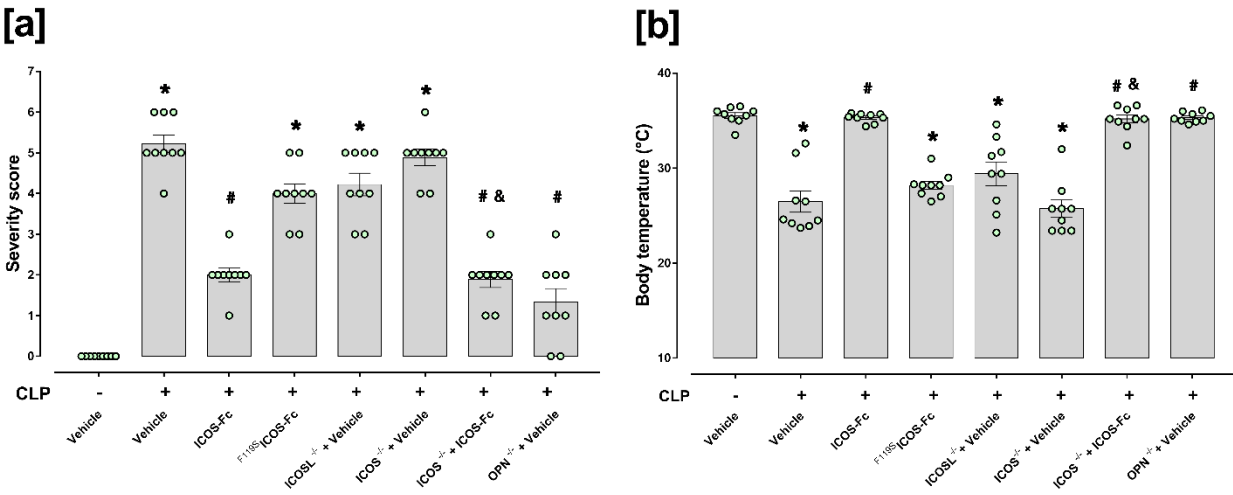
582

Figure 1



583

FIGURE 2



584

FIGURE 3

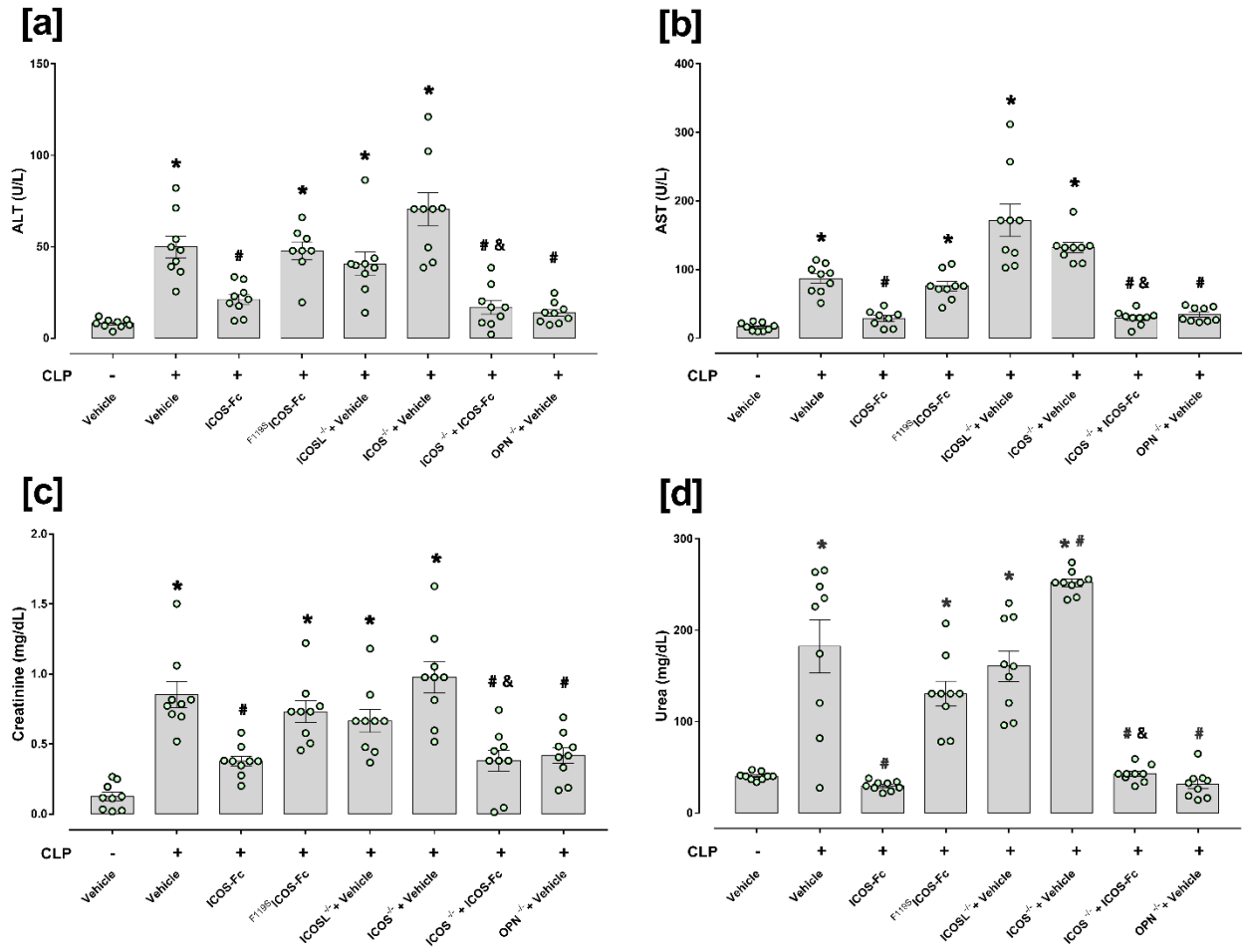


FIGURE 4

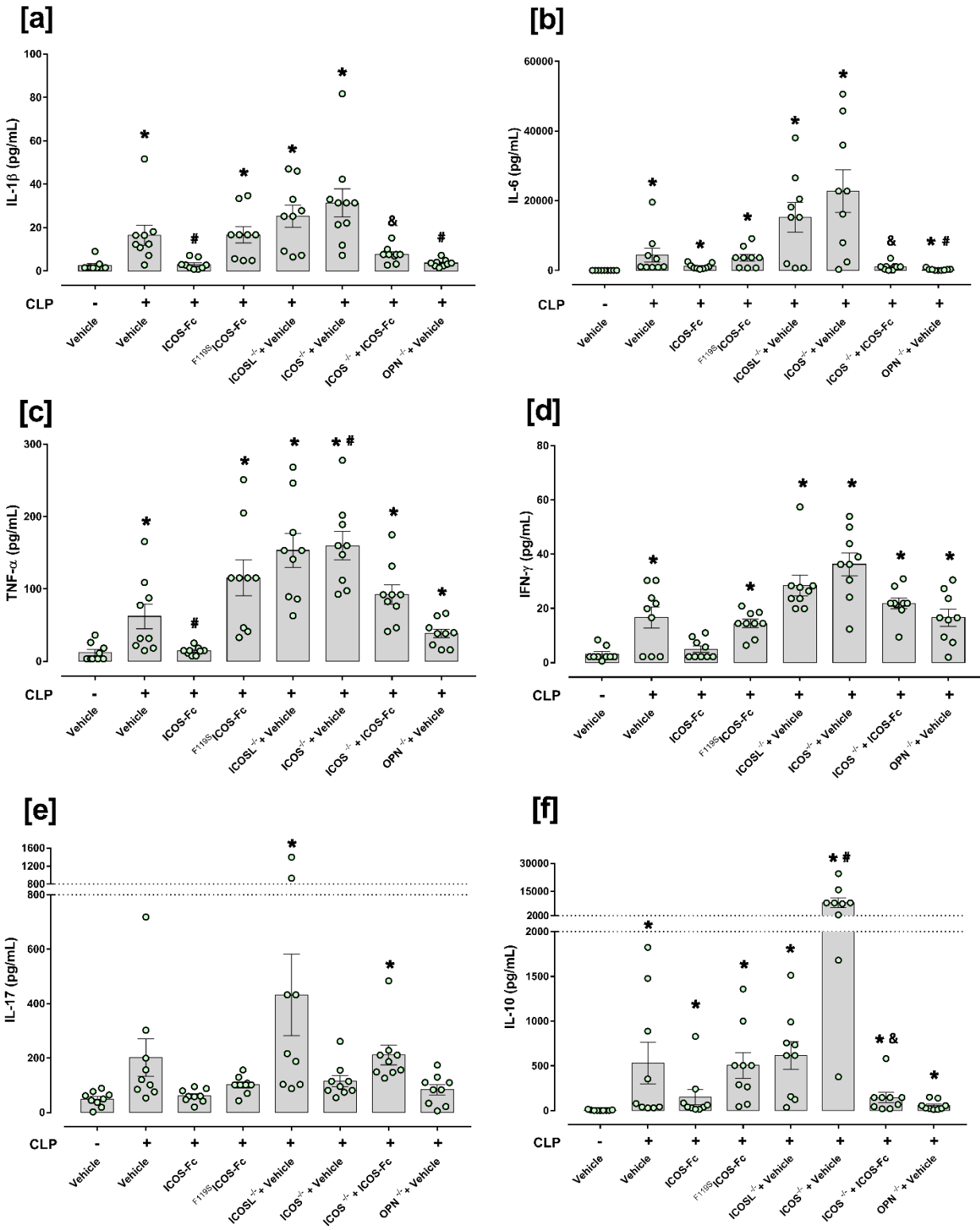
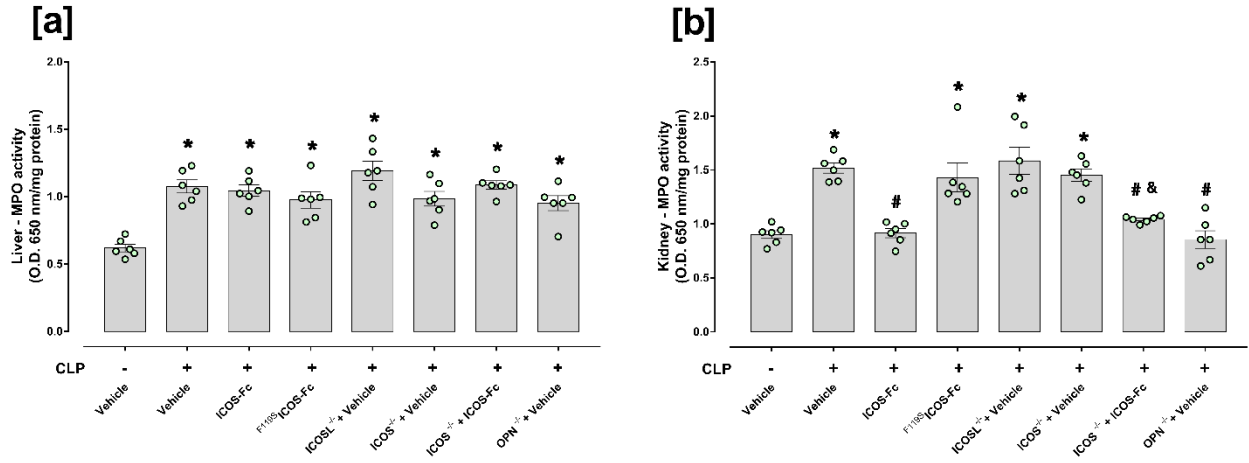


FIGURE 5



587

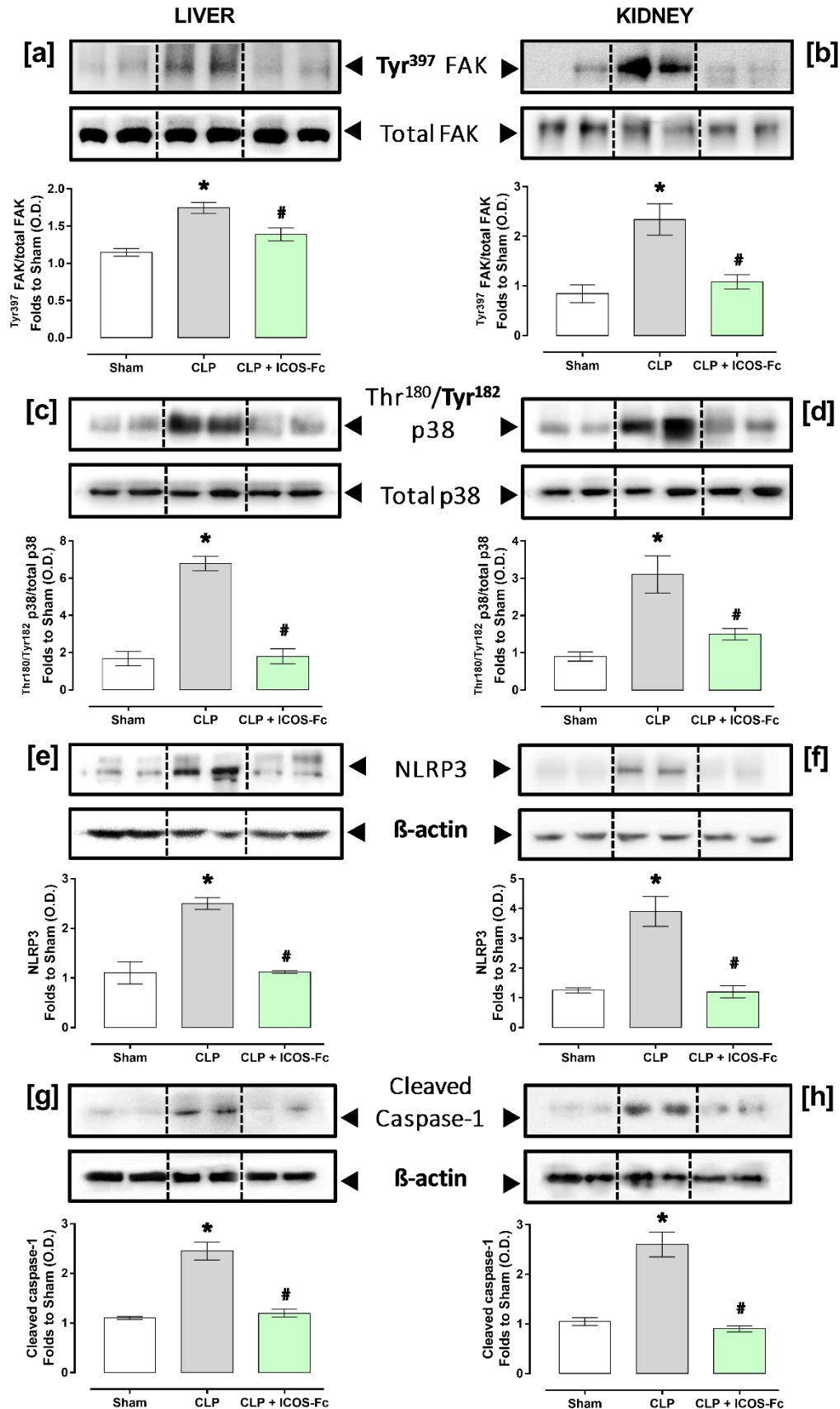
FIGURE 6

Figure 7

